Received: 29 July 2023 | Accepted: 8 September 2023

DOI: 10.1002/ecs2.4707

ECOSPHERE
AN ESA OPEN ACCESS JOURNAL

ARTICLE

Special Feature: Dynamic Deserts

Hillslope to channel hydrologic connectivity in a dryland ecosystem

Zachary T. Keller[1,2] | **Enrique R. Vivoni**[1,3] | **Charles R. Kimsal**[1] | **Agustín Robles-Morua**[3,4] | **Eli R. Pérez-Ruiz**[1,5]

[1]School of Earth and Space Exploration, Arizona State University, Tempe, Arizona, USA

[2]Surface Water Resources, Salt River Project, Tempe, Arizona, USA

[3]School of Sustainable Engineering and the Built Environment, Arizona State University, Tempe, Arizona, USA

[4]Departamento de Ciencias del Agua y Medio Ambiente, Instituto Tecnológico de Sonora, Ciudad Obregón, Mexico

[5]Departamento de Ingeniería Civil y Ambiental, Universidad Autónoma de Ciudad Juárez, Ciudad Juárez, Mexico

Correspondence
Enrique R. Vivoni
Email: vivoni@asu.edu

Funding information
Jornada Basin Long-Term Ecological Research Program, Grant/Award Number: DEB 2025166; Salt River Project

Handling Editor: Niall P. Hanan

Abstract

Hydrologic connectivity refers to the processes and thresholds leading to water transport across a landscape. In dryland ecosystems, runoff production is mediated by the arrangement of vegetation and bare soil patches on hillslopes and the properties of ephemeral channels. In this study, we used runoff measurements at multiple scales in a small (4.67 ha) mixed shrubland catchment of the Chihuahuan Desert to identify controls on and thresholds of hillslope-channel connectivity. By relating short- and long-term hydrologic records, we also addressed whether observed changes in outlet discharge since 1977 were linked to modifications in hydrologic connectivity. Hillslope runoff production was controlled by the maximum rainfall intensity occurring in a 30-min interval (I_{30}), with small-to-negligible effects of antecedent surface soil moisture, vegetation cover, or slope aspect. An I_{30} threshold of nearly 10 mm/h activated runoff propagation from the shrubland hillslopes and through the main ephemeral channel, whereas an I_{30} threshold of about 16 mm/h was required for discharge from the catchment outlet. Since storms rarely exceed I_{30}, full hillslope-channel connectivity occurs infrequently in the mixed shrubland, leading to <2% of the annual precipitation being converted into outlet discharge. Progressive decreases in outlet discharge since 1977 could not be explained by variations in precipitation metrics, including I_{30}, or the process of woody plant encroachment. Instead, channel modifications from the buildup of sediment behind measurement flumes may have increased transmission losses and reduced outlet discharge. Thus, alterations in channel properties can play an important role in the long-term (45-year) variations of rainfall–runoff dynamics of small desert catchments.

KEYWORDS
catchment hydrology, Chihuahuan Desert, environmental sensor network, ephemeral channels, hillslope hydrology, shrubland, Special Feature: Dynamic Deserts, streamflow

INTRODUCTION

The hydrologic connectivity between hillslopes and channels is important for transporting water, dissolved substances, and particulates across landscapes (e.g., Bracken et al., 2013; Jencso et al., 2009; Okin et al., 2018; Stieglitz et al., 2003). In dryland ecosystems, where water is both a limiting resource and a transport vector, overland flow resulting from intense precipitation events is the primary means for connecting hillslopes to channels (e.g., Okin et al., 2015; Schreiner-McGraw & Vivoni, 2017; Wilcox et al., 2003). This transport is mediated by the spatial arrangement of vegetation and bare soil patches that occur on a soil-geomorphic template which determines overland pathways (Monger & Bestelmeyer, 2006; Newman et al., 2006; Rango et al., 2006). Higher hydrologic connectivity occurs when runoff-producing intercanopy spaces are arranged in paths leading to downslope transport. In contrast, vegetation patches with higher infiltration capacities typically serve as runoff sinks (Seyfried & Wilcox, 1995), thereby reducing connectivity (Rossi et al., 2018). If changes in vegetation composition and structure or in the soil and topographic properties of a landscape occur, a reorganization of hydrologic connectivity is possible (e.g., Stewart et al., 2014; Yetemen et al., 2015; Zhou et al., 2013).

Runoff generation in dryland ecosystems occurs primarily when high rainfall intensities exceed the soil infiltration rate (Beven, 2002). Intercanopy spaces with bare soil, gravel or stone cover (e.g., desert pavement), and exposed rock have been shown to produce high amounts of infiltration-excess or Hortonian runoff occurring frequently after storms (e.g., Abrahams et al., 1995; Kampf et al., 2018; Puigdefabregas, 2005). In contrast, vegetation patches whose soils are characterized by higher porosity and hydraulic conductivity have a lower runoff potential (Leite et al., 2020; Ludwig et al., 2005; Schlesinger et al., 1999). As a result, dryland hillslopes with a spatial arrangement of intercanopy spaces and vegetation patches have areas that preferentially produce and reinfiltrate runoff, respectively. This leads to a well-known spatial scaling effect. As the hillslope length or area grows, a lower amount of runoff is produced downslope in response to a higher opportunity for reinfiltration to occur within the hillslope (e.g., Parsons et al., 2006; Wilcox et al., 2003). This is due to runoff losses within vegetation patches or in downstream bare soil areas that retain infiltration capacity. In cases where the spatial arrangement of plant and intercanopy patches promotes hydrologic connectivity, Wilcox et al. (2003) referred to these as "nonconserving" hillslopes with respect to water and sediment.

Less attention has been paid to the downstream connectivity between hillslopes and channels in dryland ecosystems. Indeed, most observational studies have focused either on hillslope runoff production (e.g., Abrahams et al., 1995; Gutiérrez-Jurado et al., 2013; Ludwig et al., 2005; Wilcox et al., 2003) or on channel flooding and losses (e.g., Abdulrazzak, 1995; Goodrich et al., 1997; Shanafield & Cook, 2014; Wainwright et al., 2002). In drylands with complex arrangements of hillslopes and channels, scaling issues identified by Wilcox et al. (2003) in hillslopes likely apply up to the area of small catchments that include channels. For instance, Schreiner-McGraw and Vivoni (2017) found that a first-order channel transformed runoff produced in upstream hillslopes depending on the event size. For small runoff events, the channel stored hillslope runoff in its sandy bottom and hydrologic connectivity was interrupted. In contrast, large hillslope runoff events overwhelmed the channel storage capacity and the connected system yielded discharge at the catchment outlet. Subsequently, Schreiner-McGraw and Vivoni (2018) used a hydrologic model in the catchment to identify that an event threshold in hillslope runoff of 6 mm was required for channel discharge through the outlet.

It should be reiterated that hillslope-channel connectivity in dryland ecosystems is poorly understood as compared with more humid settings (e.g., Jencso et al., 2009). Puigdefabregas et al. (1998) documented how infiltration-excess runoff and subsurface lateral flow interact to affect discharge, with the latter mechanism being more important for connectivity. In dryland ecosystems where Hortonian runoff dominates the hillslope response, the low amounts of soil water generally do not allow subsurface interactions to support connectivity (Schreiner-McGraw & Vivoni, 2017). In these circumstances, discharge should be very sensitive to perturbations in the spatial arrangement and composition of the mosaic of vegetation patches and intercanopy spaces. Thus, ecosystem state changes, such as woody plant encroachment (Archer et al., 2017) or the invasion of exotic grasses (Dogra et al., 2010), on hillslope surfaces are expected to alter hydrologic connectivity (Schreiner-McGraw et al., 2020). Furthermore, long-term changes in channel properties, for instance through the installation of check dams (Nichols & Polyakov, 2019), can also impact internal hydrologic processes and reorganize the catchment response.

In this study, we investigated dryland hydrologic connectivity through measurements of the hillslope runoff response to natural precipitation events and their linkage to discharge in a small catchment of the Chihuahuan Desert, New Mexico, USA. Four runoff plots in two hillslopes were designed and installed to sample different mosaics of vegetation patches and intercanopy spaces in the mixed shrubland. To extend the relevance of the work, we combined a ~2-year record of precipitation, soil moisture, and runoff observations in the hillslope plots, with

TABLE 1 Description of observed (Obs.) and estimated (Estim.) rainfall and runoff variables over different time periods.

Variable	Time period			
	1977–1985	2003–2011	2010–2021	2019–2021
Daily rainfall, P (mm/day)	Obs.	Obs.	Obs.	Obs.
Maximum 30-min rainfall intensity, I_{30} (mm/h)	Estim. from P	Estim. from P	Obs.	Obs.
Hillslope runoff, Q_{Plot} (cm^3/s)	...	...	...	Obs.
Averaged peak hillslope runoff, Q_{Hill} (cm^3/s)	Estim. from I_{30}	Estim. from I_{30}	Estim. from I_{30}	Obs.
Channel discharge, Q_{Chan} (m^3/s)	...	...	Obs.	Obs.
Outlet discharge, Q_{Out} (m^3/s)	Obs.	Obs.	Obs.	Obs.

Note: For each estimated variable, the source is provided. Variables that are not observed or estimated are shown with ellipses (...). The time period 2019–2021 represents the hillslope runoff observations during October 1, 2019, to September 15, 2021.

precipitation and outlet discharge data over three periods spanning a 45-year duration (Table 1), as afforded by the Jornada Long-Term Ecological Research (LTER) program, to make long-term inferences on the hillslope-channel connectivity. Previously, Turnbull et al. (2013) noted that the outlet discharge response in the shrub-encroached catchment varied between 1977–1985 and 2003–2011. Using a longer period and the set of new observations, we addressed the following questions: (1) What plot characteristics and rainfall factors control the hillslope runoff response? (2) Does a hillslope runoff threshold exist for discharge at the catchment outlet? (3) Can the long-term changes in the rainfall–runoff dynamics be explained by variations in hillslope-channel connectivity? In addressing these questions, we take advantage of multiscale, high-resolution, coordinated observations in the catchment and the long-term records from the Jornada LTER.

STUDY SITE

The arid experimental catchment (4.67 ha) is located in the Jornada Experimental Range (JER), ~20 km north of Las Cruces, New Mexico, USA, in the northern reaches of the Chihuahuan Desert (Figure 1). The catchment has north-, south-, and west-facing hillslopes with modest slopes (0°–6°), except along the channel banks where higher slopes are found (15°–25°). The first-order ephemeral channel drains a portion of the piedmont slope from east to west that emanates from the San Andres Mountains and is largely disconnected from deep water tables which are not subject to groundwater pumping (Schreiner-McGraw & Vivoni, 2017). Local climate is classified as a cold desert (Koppen zone BWk), with an annual average precipitation of 278 mm and a mean annual temperature of 18°C (Pérez-Ruiz et al., 2022), with most of the precipitation occurring during the North American monsoon (NAM; Adams & Comrie, 1997) between July and September. The ecosystem is a mixed shrubland consisting primarily of creosote bush (*Larrea tridentata*), honey mesquite (*Prosopis glandulosa* Torr.), mariola (*Parthenium incanum*), tarbush (*Flourensia cernua*), and snakeweed (*Gutierrezia sarothrae*), as described by Templeton et al. (2014), with a large amount of bare soil (~66%) covered in stones and gravel, often arranged as desert pavement (Monger & Bestelmeyer, 2006). Low grass cover is currently present in the catchment (4%), including bush muhly (*Muhlenbergia porteri*), tobosa grass (*Pleuraphis mutica*), and sand dropseed (*Sporobolus cryptandrus*). According to available documentation (Gibbens et al., 2005; Tromble, 1988), the process of woody plant encroachment has been stable over the study period. The study site has sandy-loam soil textures with a high gravel content, and a $CaCO_3$ layer at a depth of ~40 cm (Anderson & Vivoni, 2016).

METHODS

Environmental sensor network

Current monitoring efforts in the experimental catchment began in 2010 (e.g., Templeton et al., 2014; Vivoni et al., 2021) with the establishment of a dense network of precipitation, channel runoff, soil moisture, and soil temperature sensors, as well as meteorological, radiation, and energy flux measurements at an eddy covariance (EC) tower (Figure 1). This brief description of the network focuses on hydrologic sensors used in support of hillslope runoff measurements. Precipitation (P) was measured using up to four tipping-bucket rain gauges (TE525MM; Texas Electronics, Dallas, Texas, USA) in the catchment to construct a 30-min resolution spatial average based on Thiessen polygons. Discharge (Q) at 1- and 30-min intervals was measured at the catchment outlet using a Santa Rita supercritical runoff flume (Smith et al., 1981), a

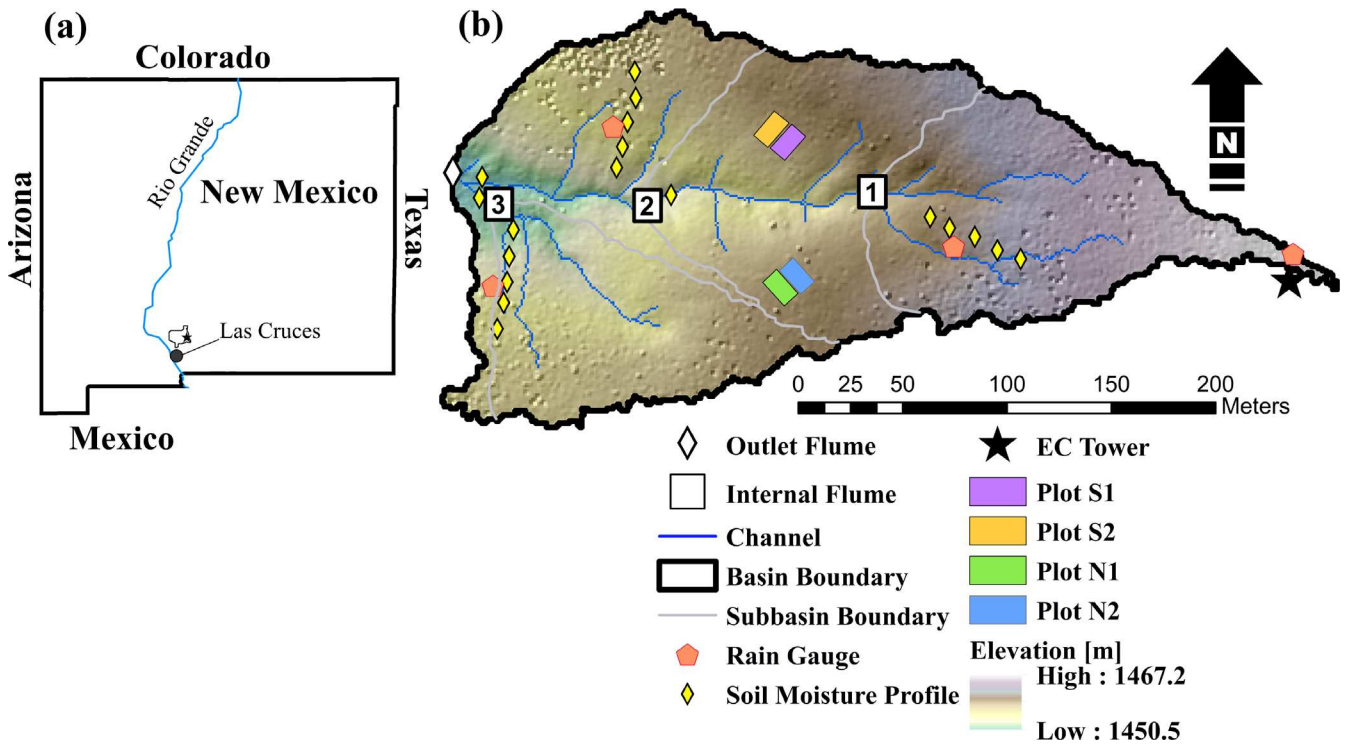

FIGURE 1 (a) Location of the study catchment (star) within the Jornada Experimental Range (polygon) in New Mexico, USA. (b) Catchment representation including: 1-m digital elevation model, channel delineation, and environmental sensor network: outlet and internal flumes, soil moisture profiles, rain gauges, eddy covariance (EC) tower, and four hillslope runoff plots (labeled S1, S2, N1, and N2 for south- [S] and north- [N] facing slopes).

pressure transducer (CS450; Campbell Scientific, Logan, Utah, USA), and an in situ calibration (Turnbull et al., 2013). In addition, long-term precipitation and outlet flume records have been in place at the site since 1977, thus allowing analyses of changes in rainfall–runoff dynamics. Since 2010, channel runoff was also obtained at three internal locations using smaller flumes (Wainwright et al., 2002), pressure transducers (CS450; Campbell Scientific), and an in situ calibration (Templeton et al., 2014). Volumetric soil moisture (θ) measurements at 30-min resolution were obtained using soil dielectric probes (Hydra Probe II; Stevens Water, Portland, Oregon, USA) organized as profiles (sensors placed at 5, 15, and 30 cm depths) in three transects along each major hillslope and at two channel locations (Figure 1b). Catchment-averaged surface soil moisture at 5 cm depth (θ_{Sur}) was obtained by weighting the locations according to elevation and aspect (Templeton et al., 2014) and used as a measure of antecedent wetness in the analysis.

Runoff plot design and measurements

Figure 1 displays the location of the four runoff plots installed in October 2019, organized into two pairs located on the north- (N1, N2) and south- (S1, S2) facing hillslopes. Each 4 × 2 m runoff plot was designed following Gutiérrez-Jurado et al. (2013). An example is shown in Figure 2a. To isolate each plot from its surroundings on three sides, polypropylene sheets (15 cm × 2.4 m) were placed 7.5 cm deep into the soil. The downslope plot boundary captured runoff using two pieces of 7.5-cm-diameter PVC pipe cut in half along their lengths, protected with a wire mesh, and inserted into a t-fitting at a 22.5° angle. The PVC system was buried ~1–2 cm into the soil to direct runoff into a 70-cm-long, fiberglass, 0.4 HS flume (Openchannelflow, Boise, Idaho, USA). Each flume had a custom-made stilling well (15 cm in diameter × 30.5 cm tall) where a CS451 pressure transducer (Campbell Scientific, Logan, Utah, USA) was housed to record water depth. Flumes and stilling wells were outfitted with covers and a wire mesh to avoid sun damage, eliminate the direct impact of precipitation, and keep wildlife out.

Processing of the hillslope runoff data followed procedures carried out at the internal and outlet flumes (Templeton et al., 2014). To reduce the variations imparted by air temperature fluctuations, a high-pass filter of 1 Hz was applied to the 1-min resolution depth values. Quality-controlled water depth values were

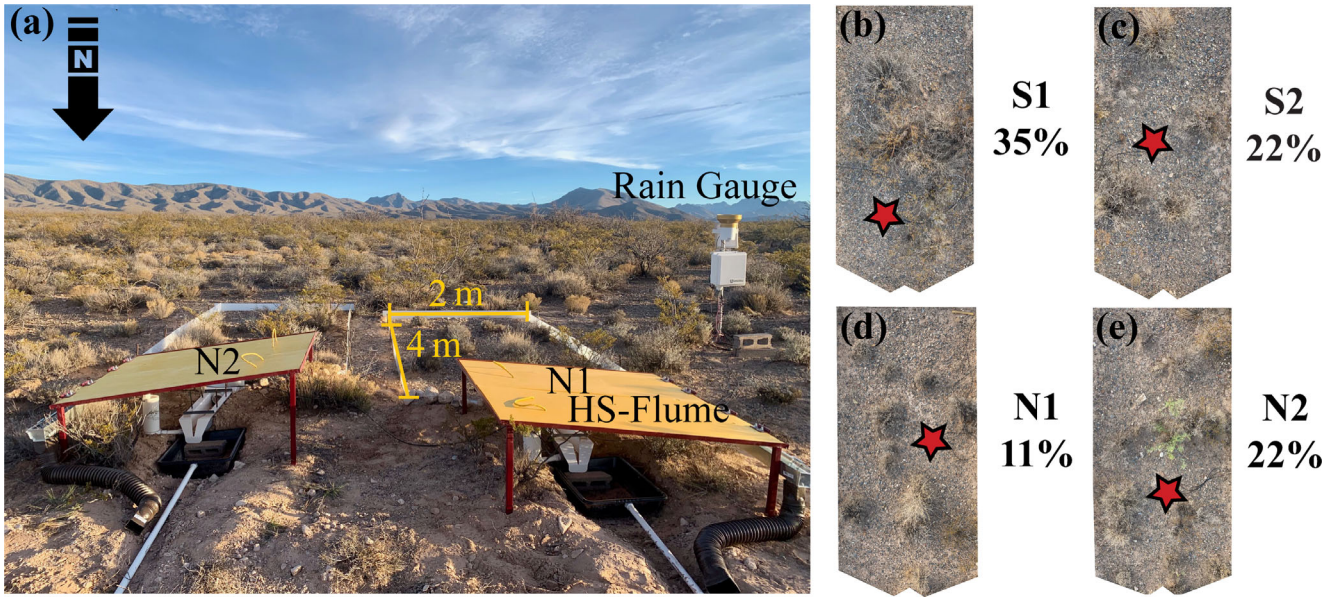

FIGURE 2 Photographs of hillslope runoff plots. (a) North-facing plots (N2 and N1) showing the plot boundaries, flow collection systems, HS flumes, stilling wells, roof coverings, and rain gauge. (b–e) Top-down image mosaics on June 27, 2021, for all plots, including estimates of vegetation fraction in percentages. One rain gauge is co-located with each pair of plots and three soil moisture sensors at different depths are buried within each plot at the sites marked with a star in (b)–(e). Photo credit: Zachary T. Keller.

converted to discharge (Q) using a polynomial equation derived for the 0.4 HS flume (Gwinn & Parsons, 1976). An analysis of measurement accuracy using the Rational method was conducted to determine the minimum detectable water depth and storm event size (Keller, 2021). This yielded that the minimum depth of 3 mm allowed flumes to detect runoff from storms that occurred with frequencies less than the 1-year return period. To complement the discharge measurements, hillslope runoff plots were equipped with a TE525MM rain gauge (one gauge per pair of plots) and with a set of three Hydra Probe II soil moisture sensors installed at 5, 15, and 30 cm depths inside each plot. Surface soil moisture at 5 cm depth (θ_{Sur}) within each plot was used as a measure of antecedent wetness in the analysis. The soil probes were installed at a single location inside each plot, as shown in Figure 2b–e.

Runoff plot siting and characterization

A spatial analysis was conducted to select the location of the runoff plots using the 1-m digital elevation model (DEM) and 1-m vegetation species map derived from an unmanned aerial vehicle image mosaic (Vivoni et al., 2014; Figure 1). We sampled only the north- and south-facing hillslopes since these occupy 39.2% and 39.1% of the catchment area, respectively (Templeton, 2011). Runoff plots were placed in the middle of each slope since soil moisture variations along the hillslopes were found to be minimal (Schreiner-McGraw & Vivoni, 2017). Located between 1458 and 1460 m, the runoff plots represent elevations that occupy about 22% of the catchment (Templeton, 2011). As shown in Figure 1, detailed site selection also accounted for (1) placement on planar hillslopes in the direction of downslope flow, (2) similar elevations in the two hillslopes in areas draining to the same channel, (3) plot siting in between two internal channel flumes, and (4) sampling of a range of vegetation and bare soil cover within the 4×2 m areas. Overhead photographs were acquired for each runoff plot during two dates representing pre-monsoon (June 27, 2021) and monsoon (August 22, 2021) conditions during the study period. Top-down images were acquired on an iPhone XR with a camera boom to cover the plot surface (see examples in Figure 2b–e) and georeferenced using four, small permanent targets placed near the plot corners. Each image mosaic was classified into bare soil and vegetated pixels using training samples and an Interactive Supervised Classification tool in ArcMap 10.6.1. The runoff plot vegetation fraction (VF) was obtained from the classified imagery on the two dates to verify that runoff plot selection sampled a range of vegetation cover conditions. Given the greening during the NAM (e.g., Schreiner-McGraw & Vivoni, 2018), VF was expected to increase over the two dates as shrubs expanded their leaf cover and grasses occupied soil spaces.

Study periods and data analyses

The study period for the runoff plot observations covered October 19, 2019, to September 15, 2021 (697 days). Due to site maintenance and the low frequency of runoff events, there were no data losses from the four plots. Observations from the site rain gauge and outlet flume extend from 1977 to 2021, with large periods of data interruptions, as documented in Turnbull et al. (2013) and Vivoni et al. (2021). Due to this, we divide the long-term record into three periods: (1) early (1977–1985), (2) intermediate (2003–2011), and (3) recent (2012–2021). The recent period has had more extensive site maintenance, a higher data quality, and a larger number of available observations of different types. For the analysis of internal and outlet runoff flumes, we use the period of June 1, 2010, to September 15, 2021, after establishment of the environmental sensor network (Templeton et al., 2014). We divided each year in the record into two 6-month seasons: cool (October–March) and warm (April–September), based on monthly mean air temperature, with the latter containing storms during the NAM (Pérez-Ruiz et al., 2022).

Precipitation, soil moisture, and discharge data from the runoff plot installations were analyzed by (1) creating high-resolution (1 or 30 min) time series, (2) counting the number and magnitude of events above specific thresholds, and (3) extracting metrics to characterize the conditions. To objectively determine the thresholds, we applied the method of Kampf et al. (2018). Similar efforts were performed for the longer records using the available rain gauge and flumes. For precipitation, we obtained daily totals (in millimeters per day) and the maximum rainfall intensity in a 30-min period, I_{30} (in millimeters per hour), used often to quantify storm intensity in regions with short-duration thunderstorms (e.g., Nearing et al., 2017; Osborn & Lane, 1969). Different I_{30} values were tested, in increments of 0.1 mm/h, to identify the threshold that correctly predicted the fraction of discharge events occurring, p_o (Kampf et al., 2018). If multiple I_{30} values yielded a similar p_o (i.e., observed agreement), the lowest value was selected as the threshold. For discharge, we derived the peak discharge (Q_{peak}) from runoff hydrographs at the four plots (Q_{Plot}, in cubic centimeters per second), at the internal channel flume downstream of the runoff plots (labeled 2 in Figure 1b, Q_{Chan}, in cubic meters per second, upstream area of 2.58×10^4 m^2 or 55% of entire watershed), and at the outlet flume (Q_{Out}, in cubic meters per second, upstream area of 4.67×10^4 m^2). The longer records at Q_{Chan} and Q_{Out} lead to more robust estimates of threshold values of I_{30}. The runoff contributions from the four plots were denoted as Q_{Hill} (in cubic centimeters per second) and average peak values, equivalent runoff depths, and total amounts were obtained as noted. To compare across plots, we estimated the event volumetric runoff ratio ($r_{Plot} = Q_{Plot}/P$) and the coefficient of the Rational method ($C_{Plot} = Q_{Plot}/I_{30}A_{Plot}$) following Moody et al. (2008), where A_{Plot} was the plot area (8 m^2). An ANOVA test was performed to determine significant differences in C_{Plot} among the runoff plots over all events in the study period, at a level of significance of $\alpha = 10\%$. Comparisons across scales of observation were obtained by normalizing peak runoff or discharge amounts by the respective upstream area.

RESULTS

Local controls on runoff plot response

Runoff plot observations spanned two cool (October–March) and two warm (April–September) seasons. To present some context for the hillslope dataset, Figure 3 shows the daily precipitation and outlet discharge records in the experimental catchment. Contrasting seasonal precipitation amounts were noted, with the years 2019–2020 composed of a wet cool season (185% of seasonal average over 2010–2021) and a dry warm season (40% of seasonal average), whereas the opposite trend occurred during 2020–2021 (28% and 123% of cool and warm season averages, respectively). The above-average precipitation in the first cool season and second warm season provided an opportunity for runoff generation. As expected, the annual and seasonal runoff ratios at the outlet (Q_{Out}/P) were very low (<2%), as also shown in Vivoni et al. (2021). A few small discharge events at the outlet occurred in the cool season of 2019–2020 indicating that runoff generation is possible outside of the NAM, in contrast to prior assumptions (Rango et al., 2003). However, the largest events were concentrated in the warm season of 2020–2021 due to the frequent number of intense storms during the NAM, with several of them exceeding 20 mm/day. From the perspective of the discharge at the catchment outlet, hydrologic connectivity appears to be low overall, consistent with Schreiner-McGraw and Vivoni (2017).

Figure 4 illustrates three selected storm events that elicited responses in the runoff plots and the internal and outlet flumes during the warm season of 2020–2021. Events represent soil and vegetation conditions during the pre-monsoon, early monsoon, and late monsoon phases of the NAM, with total event P of 37, 15, and 26 mm for June 30, July 11, and August 27, 2021, respectively. Prior to the precipitation events, θ_{Sur} averaged among the runoff plots was low, ranging from 0.05 to 0.12 m^3/m^3, for two of the events (July 11 and

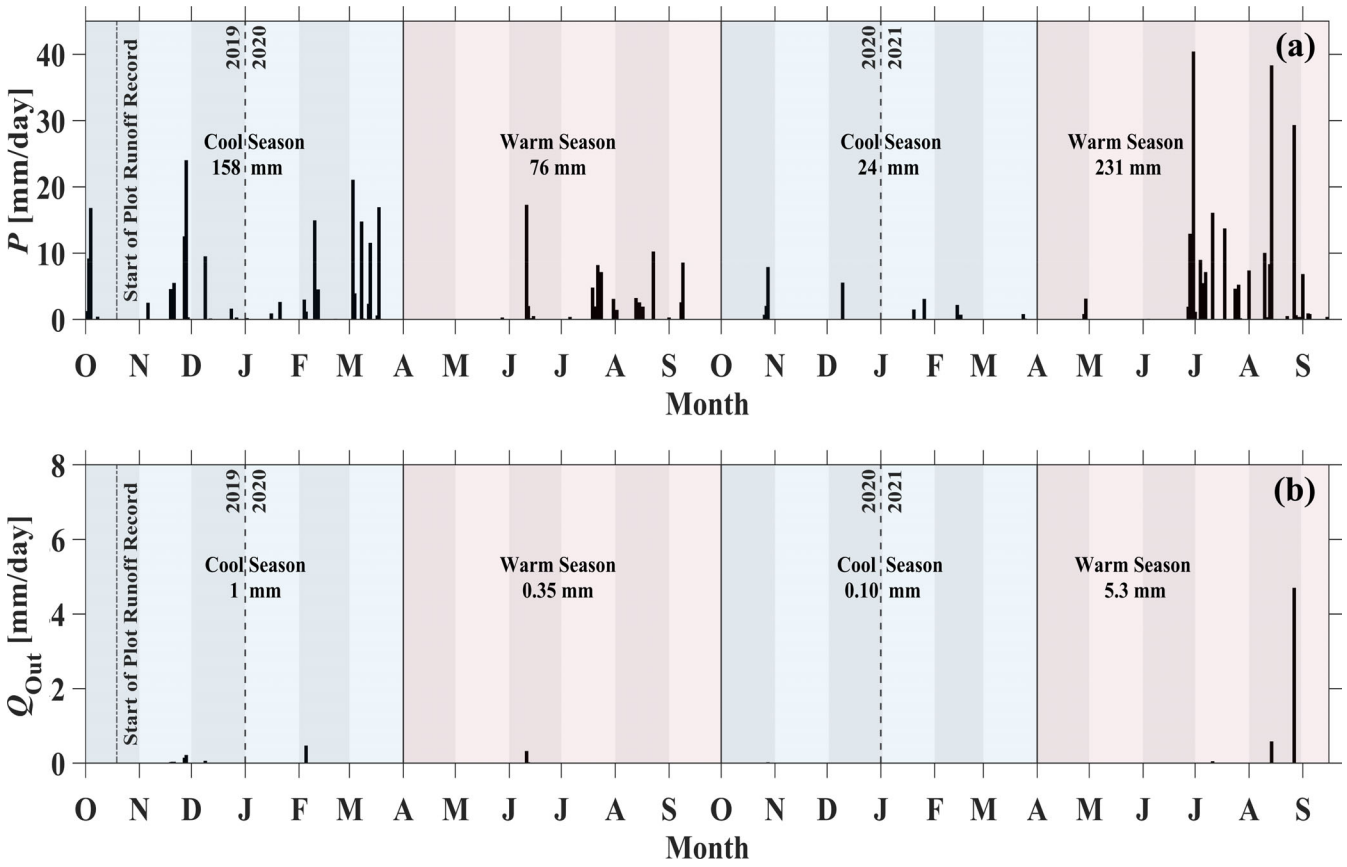

FIGURE 3 Daily observations of (a) catchment-averaged precipitation (P) and (b) outlet discharge (Q_{Out}) during the study period (October 1, 2019, to September 15, 2021), including total amounts for the two cool (October–March) and warm (April–September) seasons. Average Q_{Out}/P of 0.52%, 1.38%, and 1.35% for cool season, warm season, and annual periods.

August 27), and high for the event of June 30 (from 0.20 to 0.25 m^3/m^3). θ_{Sur} modestly increased in the 30-min period after precipitation in south-facing plots (S1, S2) and had higher increases in north-facing plots (N1, N2). High temporal (1 min) resolution records of P, Q_{Plot}, Q_{Hill}, Q_{Chan}, and Q_{Out} for the events provide useful illustrations of (1) the differences in the runoff hydrograph response among the plots, (2) the propagation or lack thereof of hillslope runoff to the channel and outlet discharge, and (3) the effect of rainfall intensity and its temporal distribution on runoff production across different scales. While each of these aspects will be detailed subsequently, it is worth mentioning that the maximum (1 min) rainfall intensity varied considerably among the events (48, 72, and 132 mm/h for June 30, July 11, and August 27, 2021) and explained runoff differences better than total event P (Keller, 2021). For higher rainfall intensities, more hillslope runoff was produced from the infiltration-excess mechanism which then increased channel discharge and connected flows through to the outlet. High-resolution channel observations are consistent with prior analyses performed for the internal and outlet flumes (Templeton et al., 2014).

Table 2 summarizes the runoff plot observations for all events during the study period (e.g., October 19, 2019, to September 15, 2021), while Figure 5 shows box and whisker plots for the peak discharge values of all events in each hillslope runoff plot (Q_{Plot}). Small differences were noted in the number of runoff events and in the average hillslope runoff peak (Q_{Plot}) among the plots, except that N2 had lowest magnitudes and corresponding values of C_{Plot} and r_{Plot}. The south-facing plots (S1 and S2) responded less frequently but exhibited the largest peaks in response to the August 27, 2021, event (Figure 4c) and had more outliers (Figure 5). Pairwise ANOVA tests of the normalized runoff response (C_{Plot}) revealed that only north-facing plots (N1 and N2) had significant differences among each other at $\alpha = 10\%$, likely due to variations in VF (Table 2). At N1, a greater amount of intercanopy spaces (lowest average VF across the two time periods of 0.22), led to a higher average C_{Plot} as compared with other runoff plots. Nevertheless, a clear effect of VF was obscured by several factors: (1) precipitation controls on runoff amount; (2) the lack of accounting for bare soil connectivity in VF as a metric for vegetation effects;

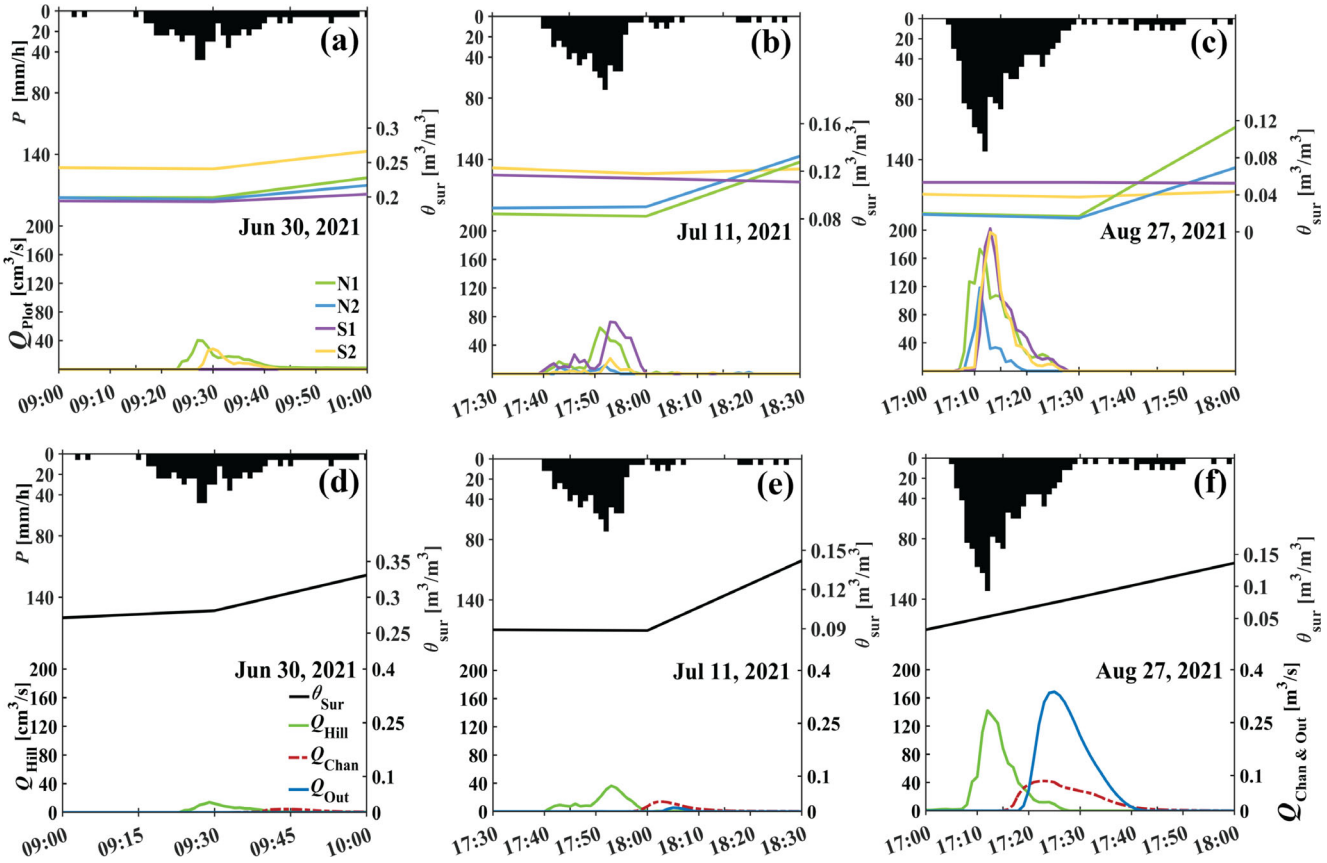

FIGURE 4 High-resolution storm event responses at hillslope runoff plots (a–c) and channel flumes (d–f) for (a, d) June 30, 2021, (b, e) July 11, 2021, and (c, f) August 27, 2021. Precipitation (P) at the north-facing runoff plots shown as an inverted axis for all events. Volumetric soil moisture in the top 5 cm (θ_{Sur}) is shown within each plot (a–c) or averaged across all plots (d–f). Discharge is shown for individual plots (Q_{Plot}, a–c) and their total contribution (labeled as Q_{Hill}, d–f) and for the internal channel flume 2 (Q_{Chan}) and outlet flume (Q_{Out}).

TABLE 2 Summary of hillslope runoff plot response and characteristics.

Plot	No. events	Q_{Plot} (cm^3/s)	C_{Plot}	r_{Plot}	VF_1	VF_2	ρ
N1	13	27 ± 44	0.05	0.08	0.11	0.33	−0.46
N2	10	13 ± 33	0.02	0.02	0.22	0.47	−0.30
S1	9	30 ± 57	0.04	0.10	0.35	0.66	−0.30
S2	8	26 ± 57	0.03	0.07	0.22	0.51	−0.59

Note: "No. events" indicates the number of runoff events over the study period (October 19, 2019, to September 15, 2021). Peak hillslope runoff (Q_{Plot}) is shown as mean ± 1 SD. C_{Plot} and r_{Plot} are the average runoff coefficient ($C_{Plot} = Q_{Plot}/I_{30}A_{Plot}$) and average runoff ratio ($r_{Plot} = Q_{Plot}/P$) during the study period, both dimensionless. Dimensionless vegetation fractions are shown for June 27, 2021 (VF_1) and August 22, 2021 (VF_2). ρ is the Pearson correlation coefficient between Q_{Plot} and θ_{Sur} for 30 min prior to the peak discharge (dimensionless).

(3) canopy interception thresholds noted for large creosote bush shrubs that influenced runoff, in particular at plot S1 (highest average VF of 0.51); and (4) variations in soil roughness and infiltration properties. Furthermore, the increase in VF with time as shrubs greened during the NAM had a small, but inconsistent, effect on C_{Plot} (Keller, 2021). For each event, we analyzed the effect of antecedent surface wetness (θ_{Sur} in the 30 min prior to runoff) on Q_{Plot}, finding a negative correlation (pooled ρ of all data of −0.35; Table 2), indicating a negligible impact with respect to moisture priming of the plots for runoff generation. We also confirmed that most infiltration depths after precipitation events only reached the top 5 cm of soil, with a low number of cases reaching 15 cm (Keller, 2021). These outcomes suggest the dominance of infiltration-excess runoff where the primary controls are related to precipitation metrics, as explored next.

Precipitation effects on hillslope-channel connectivity

We identified the effect of different precipitation thresholds on the propagation of events through the hillslope-channel system. Table 3 presents the number (or count) of precipitation (P) and runoff events at different scales in the catchment (Q_{Plot}, Q_{Chan}, and Q_{Out}) for three selected thresholds based on prior work in the study region. The three thresholds represent (1) biologically significant precipitation amounts for plant productivity in arid regions ($P \geq 5$ mm for an event; Reynolds et al., 2004); (2) hourly precipitation rates leading to outlet discharge in the catchment ($P \geq 10$ mm/h; Schreiner-McGraw & Vivoni, 2018); and (3) precipitation event sizes leading to connectivity across landscape units ($P \geq 20$ mm/day; McKenna & Sala, 2018). Since storm events during the NAM typically last less than 1 h and multiple events during a day are rare (Wainwright, 2006), these thresholds effectively have the same time span. At the low threshold of 5 mm/event, a small percentage of precipitation is converted to hillslope runoff, and then to channel and outlet discharge (32%, 25%, and 11%, respectively). At the higher 20 mm/day threshold, the hillslope-channel connectivity grows substantially, with nearly all the storm events eliciting a hillslope response and 50% of the events leading to outlet discharge. For these cases, discharge from the outlet likely continues downstream, leading to landscape-scale connectivity (Okin et al., 2018). The intermediate threshold of $P \geq 10$ mm/h resulted in 63%, 54%, and 30% of the events leading to hillslope, channel, and outlet discharge, respectively.

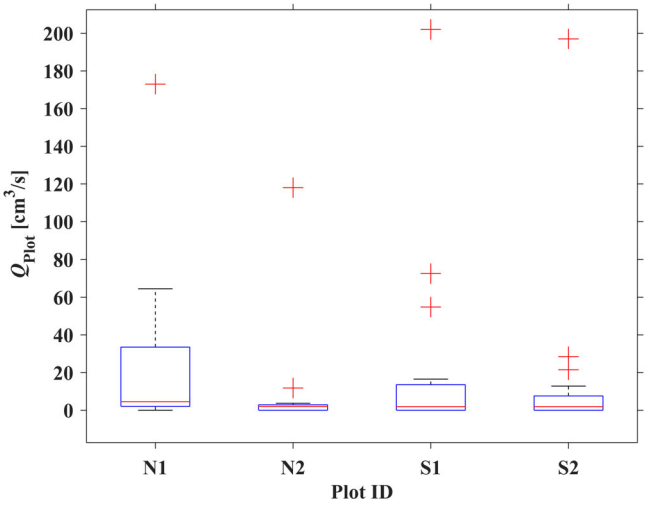

FIGURE 5 Box and whisker plots of Q_{Plot} for all events in the hillslope runoff plots (N1, N2, S1, S2) during the study period (October 1, 2019, to September 15, 2021). In each box and whisker plot, red lines are the median, blue boxes indicate the 25th and 75th percentiles, whiskers extend to extreme points not considered outliers, and outliers are plotted using red crosses.

To explore this further, Figure 6 presents the relations between the maximum rainfall intensity (I_{30}) and peak discharge at the three scales of observations (Q_{Plot}, Q_{Chan}, and Q_{Out}). Note that I_{30} is distinct from the precipitation amounts tested in Table 3. For each case, θ_{Sur} is shown through the symbol size, obtained within the runoff plots for Q_{Plot} or averaged across the sensor network for Q_{Chan} and Q_{Out}. Over their shorter record, runoff plots exhibited a threshold behavior in runoff response at $I_{30} = 9.3$ mm/h (observed agreement, p_o of 87.2%), obtained from the method of Kampf et al. (2018), and with a negligible sensitivity to antecedent wetness. Consistent with this, both Q_{Chan} and Q_{Out} show a good correspondence with I_{30} threshold values of 9.6 mm/h ($p_o = 92.6\%$) and 16.1 mm/h ($p_o = 93.2\%$), although a few events (<5) over the longer records do not conform to this behavior. These outliers were identified as resulting from low-intensity, long-duration winter storm events. Short storm durations at the site result in I_{30} magnitudes that are similar to hourly and daily totals (as discussed in the next section). As shown previously, the antecedent surface wetness had no effect on runoff production (Table 2), with the largest peak discharges in Q_{Plot}, Q_{Chan}, and Q_{Out} often associated with low θ_{Sur}.

TABLE 3 Hydrologic connectivity from hillslope runoff plots to the catchment outlet.

	Threshold ≥5 mm/event				Threshold ≥10 mm/h				Threshold ≥20 mm/day			
Plot	P	Q_{Plot}	Q_{Chan}	Q_{Out}	P	Q_{Plot}	Q_{Chan}	Q_{Out}	P	Q_{Plot}	Q_{Chan}	Q_{Out}
N1	32	13	11	4	11	9	9	4	4	4	2	2
N2	32	10	7	4	11	7	5	4	4	3	2	2
S1	30	9	7	3	12	7	6	3	4	3	2	2
S2	30	8	6	3	12	6	5	3	4	4	3	2

Note: Event counts (number) are shown for each of the following observations: precipitation (P), hillslope runoff (Q_{Plot}), channel runoff (Q_{Chan}), and outlet discharge (Q_{Out}) during the study period (October 19, 2019, to September 15, 2021), for different thresholds: $P \geq 5$ mm for event; $P \geq 10$ mm/h as hourly rate during event; and $P \geq 20$ mm/day as daily sum. $P \geq 10$ mm/h results in similar hydrologic connectivity as obtained for $I_{30} \geq 10$ mm/h.

Notably, the hillslope-channel system appears to be well connected for maximum rainfall intensities at 30 min exceeding nearly 10 mm/h (Table 3), which result in similar outcomes as $P \geq 10$ mm/h. Note that 45%–82% of the storm events with $I_{30} \geq 10$ mm/h lead to Q_{Plot} and Q_{Chan}, while only 25%–36% of the storm events result in Q_{Out}. We attribute the similar I_{30} thresholds for Q_{Plot} and Q_{Chan} to their proximity, while differences with Q_{Out} indicate that channel transmission losses require larger events for hydrologic connectivity to occur (Schreiner-McGraw & Vivoni, 2017). The derived threshold values are consistent with those obtained in other small arid catchments (Kampf et al., 2018; Moody et al., 2008; Osborn & Lane, 1969; Polyakov et al., 2010).

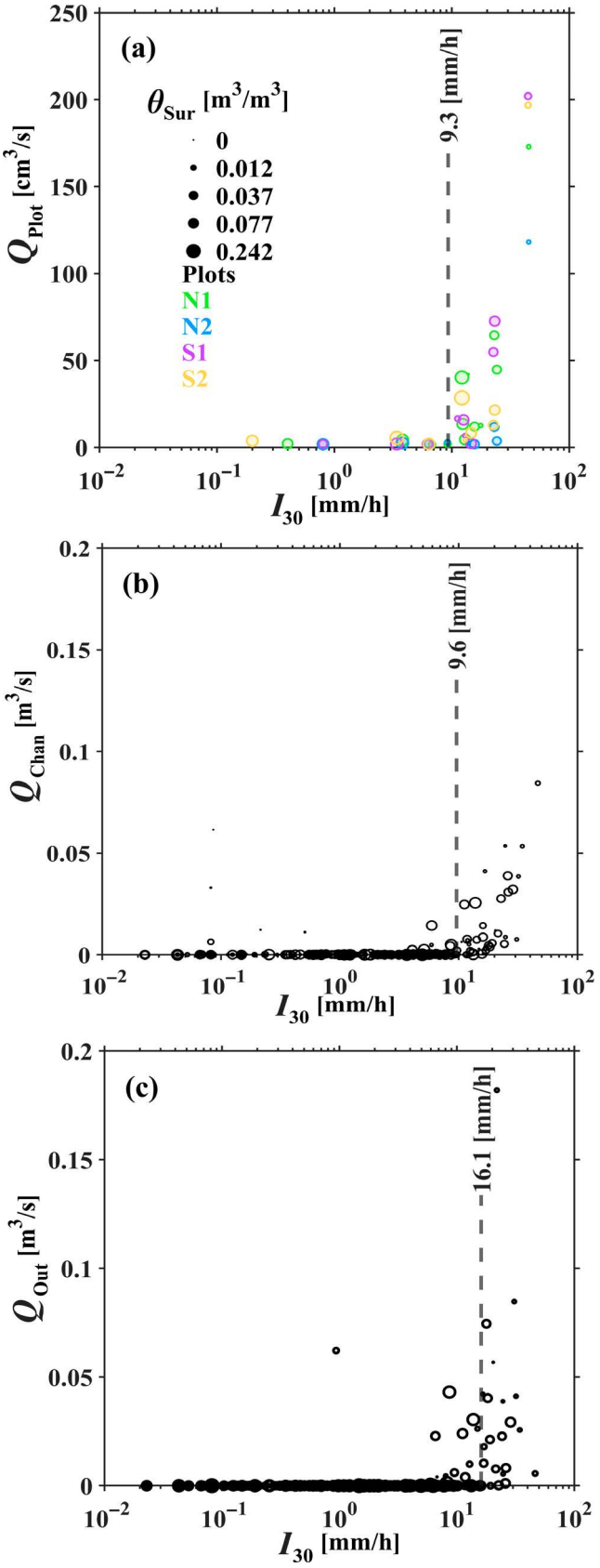

Through a modeling exercise in the catchment, Schreiner-McGraw and Vivoni (2018) identified a threshold in hillslope runoff of 6 mm/event that led to outlet discharge. This threshold referred to the hillslope runoff beyond which outlet discharge could be expected, though there were a few cases of Q_{Out} near zero despite $Q_{Hill} \geq 6$ mm. Below this threshold, hillslope runoff was mostly absorbed in the channel through transmission losses (e.g., infiltration and storage in sandy channel bottoms), with $Q_{Out} \leq 0.25$ mm. In their study, hillslope runoff plots were not available in the catchment, such that hydrologic connectivity was only derived from the model simulations. Figure 7 shows the relation between average hillslope runoff in the plots and the outlet discharge obtained during the study period, along with an exponential regression of the dataset used as a visual aid. In each case, the runoff volume for each event was normalized by the area of a runoff plot and the catchment, respectively, to obtain an equivalent runoff depth. While the total number of events is limited (Table 3), the observations indicate that the model-derived threshold is a plausible description of the hydrologic processes occurring in the catchment, such that large amounts of Q_{Out} occur after $Q_{Hill} \geq 6$ mm. Additional measurements of hillslope runoff events in the range of 3–7 mm in depth are desirable to more precisely quantify the threshold and to test whether an exponential or a piecewise linear relation would be more suitable to describe the hydrologic connectivity in the hillslope-channel system.

FIGURE 6 Relations between rainfall intensity (I_{30}) and peak discharge at: (a) hillslope runoff plots (Q_{Plot}), (b) internal channel flume (Q_{Chan}), and (c) outlet flume (Q_{Out}). Symbol sizes represent volumetric soil moisture in the top 5 cm surface (θ_{Sur}) prior to each runoff event. Runoff plots are labeled with different colors in (a). Vertical dashed lines represent the derived I_{30} threshold at each scale. Note that the study period in (a) is October 1, 2019, to September 15, 2021, while (b) and (c) include events from June 1, 2010, to September 15, 2021.

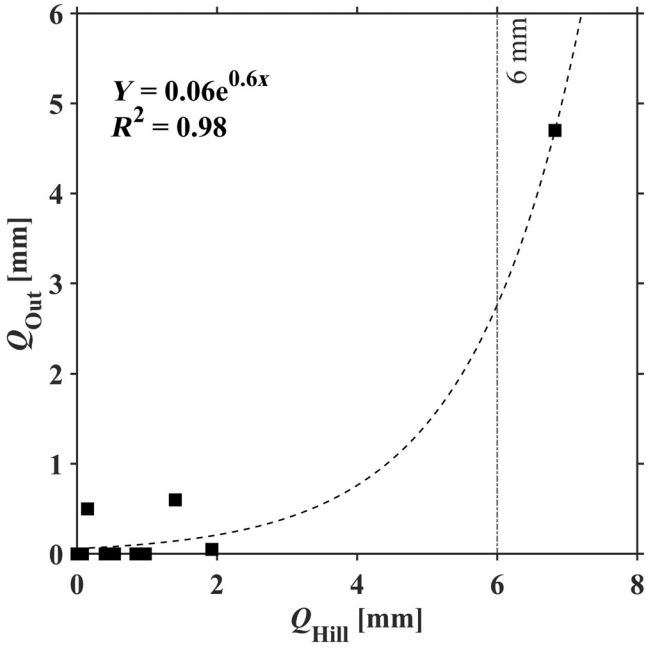

FIGURE 7 Relation between hillslope runoff averaged across the four plots and the outlet discharge for all events from October 1, 2019, to September 15, 2021. Runoff volumes have been normalized by their respective areas (8 m^2 for the runoff plots and 4.67 ha for the outlet). An exponential regression of the form $Y = ae^{bx}$ with the coefficient of determination (R^2) value is shown by the dashed line as a visual aid. The vertical line is the model-derived hillslope runoff threshold for outlet discharge (Schreiner-McGraw & Vivoni, 2018).

Long-term changes in hillslope-channel connectivity

Recent precipitation and runoff observations were used to derive relations to estimate changes in the hillslope-channel connectivity over a 45-year duration (Table 1). Over the longer period, only daily precipitation and outlet discharge were available for those events producing runoff (Turnbull et al., 2013). As a result, we derived a linear relation between I_{30} and daily P ($P = 0.93I_{30} + 0.06$, $R^2 = 0.77$; Figure 8a) for the warm season to extrapolate the controls of I_{30} on hillslope runoff to periods with only daily totals. The regression has parameters indicating the similarity of daily P to I_{30} (i.e., coefficient near unity, intercept near zero), indicating that sub-hourly and daily precipitation totals are similar due to short storm durations. However, there is observed variability between daily P and I_{30} not captured by the linear regression ($R^2 = 0.77$), which introduces uncertainty in subsequent analyses. We limited the linear relation to the warm season due to its preponderant control on hillslope runoff generation, whereas the cool season exhibited a slightly lower I_{30} for a given daily P ($P = 1.45I_{30} + 0.03$, $R^2 = 0.66$ for the cool season). We then related measurements of I_{30} and the average peak discharge from the runoff plots (Q_{Hill}) during the study period. Averaging the peak response from the hillslope runoff plots was deemed appropriate to capture the variability in vegetation cover within hillslopes in the catchment. A piecewise linear relation between I_{30} and Q_{Hill} was obtained (Figure 8b), confirming that a threshold behavior is present in Q_{Hill} at I_{30} near 10 mm/h, with a linear regression of $Q_{Hill} = 3.55I_{30} - 35.50$ ($R^2 = 0.88$) for $I_{30} \geq 10$ mm/h. The combination of these two relationships (Figure 8a,b) allows estimating Q_{Hill} from the readily available daily P in the catchment ($Q_{Hill} = 3.82P - 35.71$, for $P \geq 9.36$ mm). Considering that woody plant encroachment has stabilized (Gibbens et al., 2005), estimates of Q_{Hill} are likely robust over the 45-year duration of the record (1977–2021). Similarly, the P and I_{30} relation obtained over 2010–2021 is assumed invariant over the longer period as several multiyear precipitation cycles are sampled (Peters et al., 2021).

Figure 9 presents the estimated Q_{Hill} obtained from daily precipitation during the three time periods in the catchment record: early (1977–1985), intermediate (2003–2011), and recent (2012–2021). Despite the similar mean annual precipitation (MAP), large differences were noted in daily P among the periods (Table 4). As compared with 2003–2011, the early and recent periods had larger P and I_{30}. In response, hillslope runoff occurred at higher magnitudes in the early (1977–1985) and recent (2012–2021) periods. Nevertheless, the magnitude of the discharge events at the catchment outlet (Q_{Out}) does not track this behavior (Table 4). Instead, there is a progressive decrease in the magnitude of Q_{Out} during the 45-year period that is inconsistent with the trends in P, I_{30}, and Q_{Hill}. Figure 10 supports this comparison by presenting the variation of observed Q_{Out} with estimated I_{30} for the three periods with respect to the derived relation between Q_{Hill} and I_{30} that is assumed to be invariant in time. For comparison purposes, peak Q_{Hill} and Q_{Out} were normalized by their areas. Hillslope-channel connectivity appears to decrease over time as Q_{Hill} and Q_{Out} become further apart (i.e., black line compared with dashed lines in Figure 10 representing linear regressions of the observations), with a larger change noted from the intermediate to the recent periods, despite its shorter interval relative to the span between 1977–1985 and 2003–2011. While observed values of peak Q_{Out} versus I_{30} have variations around each regression, there is a noticeable decrease over time. Since temporal changes in outlet discharge are not explained by variations in rainfall characteristics, as proposed by Turnbull et al. (2013), or by differences in hillslope runoff (Q_{Hill}), we hypothesize that long-term modifications have occurred in the channel to

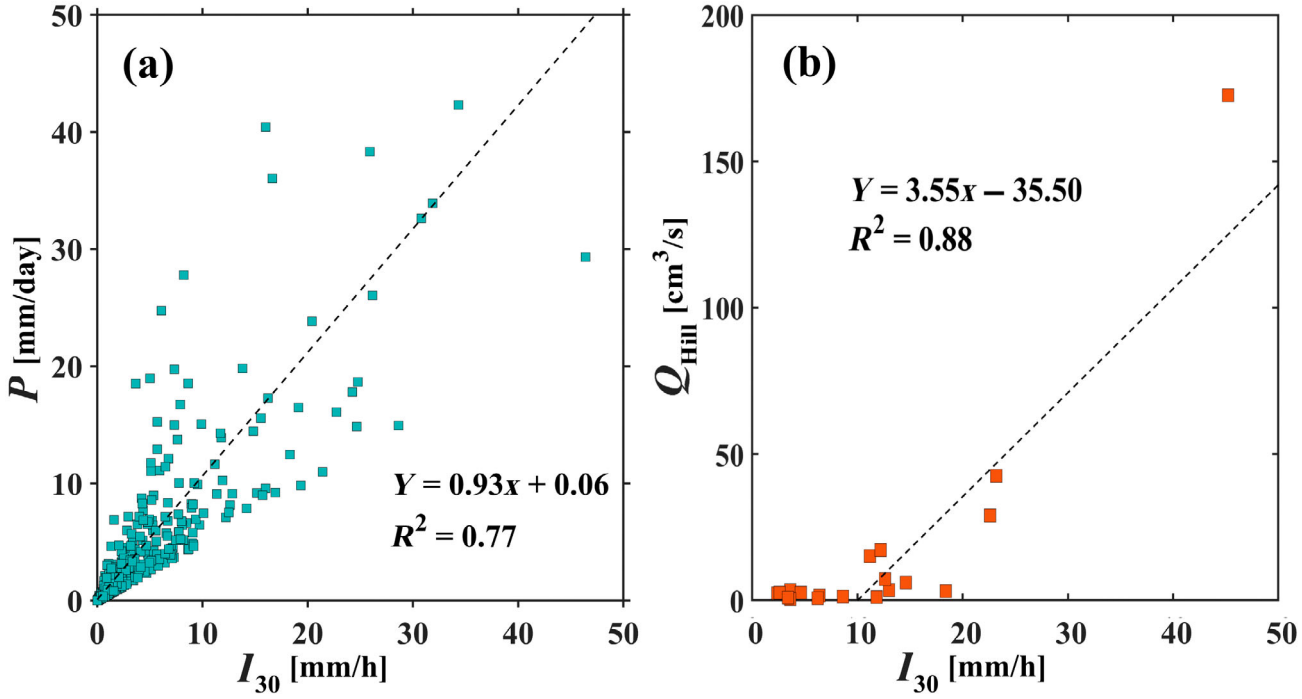

FIGURE 8 Relations between maximum 30-min rainfall intensity (I_{30}) and (a) daily precipitation (P) over June 1, 2010, to September 15, 2021, for the warm season, and (b) averaged peak hillslope runoff from all plots (Q_{Hill}) over October 1, 2019, to September 15, 2021. Dashed lines are linear regressions with equations of the form $Y = mx + b$, and coefficient of determination (R^2) values, with (b) only accounting for $I_{30} \geq 10$ mm/h.

affect the connectivity of hillslope runoff to outlet discharge.

DISCUSSION

Hillslope runoff response in mixed shrubland

The four runoff plots sampled north- and south-facing locations at the same elevation in the catchment. Hillslopes consisted of varying assemblages of woody shrubs, such as creosote bush, honey mesquite, and mariola, and intercanopy spaces covered with bare soil or stones that are characteristic of piedmont slopes in the Chihuahuan Desert (e.g., Monger & Bestelmeyer, 2006; Wainwright et al., 2002; Wondzell et al., 1996). Hillslope measurements over an ~2-year period confirmed that infiltration-excess overland flow was the primary mechanism for runoff generation, as suggested by Schreiner-McGraw and Vivoni (2017). This mechanism was identified based on: (1) infiltration depths after events that were limited to the upper 5–15 cm, (2) peak hillslope runoff amounts that were linked primarily to the maximum rainfall intensity (I_{30}), and (3) the negligible effects of antecedent wetness (θ_{Sur}) on runoff

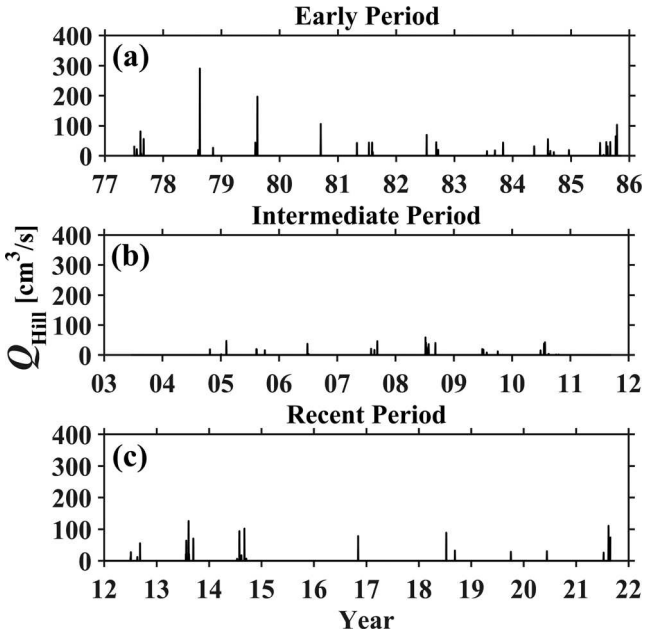

FIGURE 9 Estimated average peak hillslope runoff from plots (Q_{Hill}) for: (a) early (1977–1985), (b) intermediate (2003–2011), and (c) recent (2012–2021) periods.

production. The limited role of θ_{Sur} was likely due to the high evapotranspiration amounts in the summer

TABLE 4 Statistics of observed daily precipitation (P), estimated maximum rainfall intensity in 30 min (I_{30}), estimated peak hillslope runoff (Q_{Hill}), and observed peak outlet discharge (Q_{Out}) over three periods (mean ± 1 SD).

Period	MAP (mm/year)	P (mm/day)	I_{30} (mm/h)	Q_{Hill} (cm^3/s)	Q_{Out} (m^3/s)
1977–1985	293	16 ± 14	18 ± 3	46 ± 8	0.12 ± 0.23
2003–2011	306	6 ± 5	7 ± 2	19 ± 3	0.03 ± 0.13
2012–2021	273	11 ± 11	14 ± 2	45 ± 5	0.02 ± 0.28

Note: MAP is the mean annual precipitation over the indicated period.

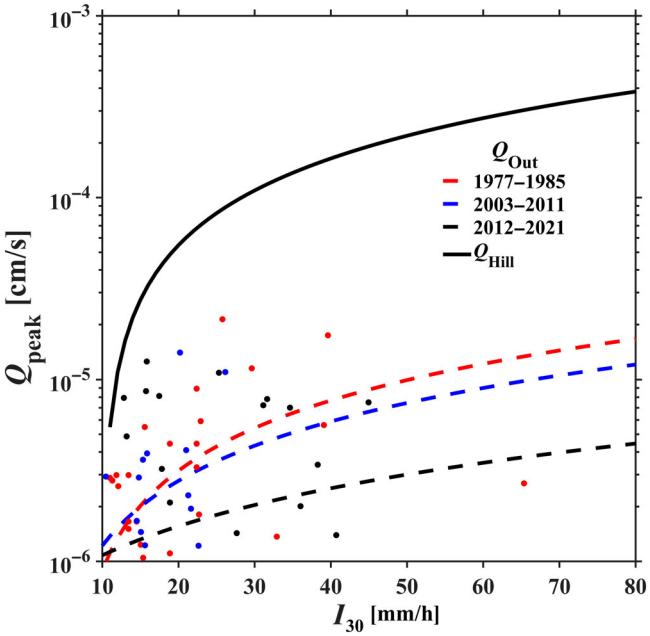

FIGURE 10 Relations between maximum rainfall intensity (I_{30}) and normalized peak discharge (Q_{peak}) estimated from hillslopes (Q_{Hill}, solid line) and observed at the catchment outlet (Q_{Out}), with the latter case shown over the three time periods. Colored dots represent individual events for each period, while the dashed lines depict linear regressions.

(~2–4 mm/day; Pérez-Ruiz et al., 2022), leading to a rapid drying of the surface soils. Similar conclusions were obtained by Kampf et al. (2018) for small watersheds in the Sonoran Desert.

A threshold in hillslope runoff production occurs when I_{30} exceeds about 10 mm/h, consistent with studies in other arid regions (e.g., Moody et al., 2008; Polyakov et al., 2010). We noted differences in hillslope runoff across the plots among individual storm events (Figure 4a–c). Shrub cover, as assessed through the VF, did not explain runoff plot differences well due to the confounding effects of precipitation and other factors by which shrubs can affect runoff, such as the arrangement of bare soil connectivity (Okin et al., 2015) and thresholds in canopy interception (Abrahams et al., 2003). In addition, the low number of runoff plots established at similar elevations along two hillslopes and the relatively few hillslope runoff events during the short record limited the sampling of the potential runoff controls of VF. In contrast to another hillslope runoff study in the Chihuahuan Desert (Gutiérrez-Jurado et al., 2013), no apparent effect of aspect was identified on runoff, likely due to the relative similarities in soil and vegetation conditions among the two hillslopes (Templeton et al., 2014). Our record, however, did not sample a large runoff-producing event, for instance, $I_{30} \geq 50$ mm/h, which would likely lead to larger differences among hillslopes, as noted by Gutiérrez-Jurado et al. (2007). Nevertheless, the sampled variability in the runoff plot characteristics and their responses (Table 2) provided an adequate basis for averaging their peak discharge to estimate the hillslope contribution to channel runoff.

Hillslope-channel connectivity in ephemeral catchment

Hillslope runoff in the form of overland flow was tracked in the main channel using downstream internal and outlet flumes. During events with higher rainfall intensity, more hillslope runoff was produced from the infiltration-excess mechanism which increased channel discharge at internal flumes and connected flows through to the catchment outlet (cf. Figure 4f on August 27, 2021). The main channel is narrow along its 200 m length, with a width of only ~0.5 m at the outlet (Figure 1). Along its flow path, the main channel aggregates small rills that drain the north- and south-facing slopes. In addition to widening, the channel becomes more permeable along its path, as indurated petrocalcic horizons in upstream locations are covered by sands, pebbles, and coarse gravel at downstream sites (Templeton et al., 2014). Using soil moisture observations within the channel sediments, Schreiner-McGraw and Vivoni (2017) showed how runoff events could be stored up to depths of at least 1 m. Based on multiple datasets, the authors proposed a conceptual model for channel transmission losses whereby: (1) small hillslope runoff events are entirely captured within channel storage, and (2) large hillslope runoff events exceed channel storage capacity

and lead to discharge at the outlet. Through this analysis, we identified that a I_{30} threshold of about 10 mm/h activated hillslope runoff generation ($I_{30} = 9.3$ mm/h, $p_o = 87.2\%$) and propagated to the downstream flume ($I_{30} = 9.6$ mm/h, $p_o = 92.6\%$), whereas a larger I_{30} threshold of 16.1 mm/h ($p_o = 93.2\%$), was required for full hydrologic connectivity to the catchment outlet. Precipitation events with I_{30} larger than 10 mm/h but smaller than 16 mm/h generate hillslope and internal channel runoff but are captured through channel transmission losses. Those events with $I_{30} \geq 16$ mm/h exceed the channel storage capacity and produce outlet discharge. This is consistent with Kampf et al. (2018) who found threshold values of maximum 60-min rainfall intensity from 5 to 13 mm/h leading to runoff in arid sites of similar area (4.9–6.1 ha) in the Sonoran Desert. In addition, a hillslope runoff threshold leading to outlet discharge (6 mm/event), as found in the modeling effort of Schreiner-McGraw and Vivoni (2018), was corroborated as plausible. Additional data are needed to refine the value of the hillslope runoff threshold and identify the functional form of the relation (i.e., piecewise linear or exponential). Overall, the full hydrologic connectivity in the hillslope-channel system of the catchment was achieved infrequently and a large proportion of the hillslope runoff events led only to channel transmission losses.

Long-term changes in rainfall–runoff dynamics

Hillslope runoff measurements were used to derive relations with daily precipitation that extended the findings back to when the outlet flume and rain gauge were installed in 1977 and records of runoff-producing events are available. This involved establishing a piecewise linear relation between peak hillslope runoff and I_{30} (from October 19, 2019, to September 15, 2021, using the runoff plots) and a linear relation between warm season daily P and I_{30} (from June 1, 2010, to September 15, 2021, when high-resolution precipitation data were available). A small difference was noticed between warm and cool season events when analyzing the relations between daily P and I_{30}, with the warm season playing a dominant role, as expected. While the long-term measurements were not continuous, three separate periods, each of 9 or 10 years in duration, were available. Turnbull et al. (2013) identified that the rainfall–runoff dynamics varied between the first two periods and attributed this to differences in the distribution of daily rainfall such that higher runoff-producing events occurred. When comparing the three periods, however, a progressive decrease in time in the outlet discharge cannot be fully explained by variations in precipitation metrics, including I_{30}. Instead, we hypothesize that the reductions in catchment discharge might be related to modifications in the channel properties occurring over the 45-year period. More specifically, the installation of the outlet flume prior to 1977 and the internal flumes in 2010 have notably led to the retention of sediment behind them, leading to wider, deeper, and sandier internal channels that have the capacity to absorb and transmit water through the subsurface. In effect, the measurement devices could function as grade control structures which lead to the retention of sediment and the detention of water (e.g., Galia & Skarpich, 2017; Norman et al., 2022; Wohl, 2006). Similar effects occur when check dams or rock retention structures are installed to retain sediments in ephemeral channels (e.g., Nichols & Polyakov, 2019; Norman et al., 2019). As a result, the full hydrologic connectivity in the hillslope-channel system appears to have been reduced over time, in part due to the channel modifications created by the flume installations themselves.

CONCLUDING REMARKS

In this study, we investigated the hillslope-channel hydrologic connectivity in an ephemeral catchment of the Chihuahuan Desert. Using observations that spanned a 45-year period, the changing nature of the catchment response was quantified by establishing relations between recent sensor network data and sparser long-term records. Hillslope runoff inputs to channels were influenced mainly by the maximum rainfall intensity over short durations, with limited controls of seasonal changes in vegetation cover or antecedent wetness. A precipitation threshold of about 16 mm/h in 30 min was necessary in the recent record for establishing full hydrologic connectivity from hillslopes to the catchment outlet. However, given the absence of long-term (45-year) trends in precipitation or woody shrub cover, hillslope hydrologic processes could not explain the reductions in outlet discharge noted in the observational record. We hypothesize that the hillslope-channel connectivity has been progressively changed through modifications in the channel conditions from the installation of flumes prior to 1977 and in 2010. Additional efforts are required to ascertain if the detained water through channel transmission losses leads to groundwater recharge or bypasses the grade control structures to augment runoff downstream.

ACKNOWLEDGMENTS

We thank John Anderson, David Thatcher, and staff members of the Jornada Experimental Range. This work

was supported by funding from the National Science Foundation to New Mexico State University for the Jornada Basin Long-Term Ecological Research (LTER) Program (DEB 2025166). We acknowledge the in-kind and financial support from Salt River Project. We thank Greg Maurer from the Jornada LTER for his contributions to the dataset documentation. We are grateful to R.C. Templeton, C.A. Anderson, and A.P. Schreiner-McGraw for their field support. Two anonymous reviewers provided excellent comments that helped improve an early version of the work.

CONFLICT OF INTEREST STATEMENT

The authors declare no conflicts of interest.

DATA AVAILABILITY STATEMENT

Data (Turnbull et al., 2020; Vivoni et al., 2022) are available from the Environmental Data Initiative: https://doi.org/10.6073/pasta/1ddf31fd56d97f4b2817b2e17d683bbc and https://doi.org/10.6073/pasta/759f2f1bc29df9bd15a9a9bfd6a15470.

ORCID

Enrique R. Vivoni https://orcid.org/0000-0002-2659-9459

REFERENCES

Abdulrazzak, M. J. 1995. "Losses of Flood Water from Alluvial Channels." *Arid Land Resources Management.* 9(1): 15–24. https://doi.org/10.1080/15324989509385870.

Abrahams, A. D., A. J. Parsons, and J. Wainwright. 1995. "Effects of Vegetation Change on Interrill Runoff and Erosion, Walnut Gulch, Southern Arizona." *Geomorphology* 13(1–4): 37–48. https://doi.org/10.1016/0169-555X(95)00027-3.

Abrahams, A. D., A. J. Parsons, and J. Wainwright. 2003. "Disposition of Rainwater under Creosotebush." *Hydrological Processes* 17(13): 2555–66. https://doi.org/10.1002/hyp.1272.

Adams, D. K., and A. C. Comrie. 1997. "The North American Monsoon." *Bulletin of the American Meteorological Society* 78: 2197–2213. https://doi.org/10.1175/1520-0477(1997)078%3C2197:TNAM%3E2.0.CO;2.

Anderson, C. A., and E. R. Vivoni. 2016. "Impact of Land Surface States within the Flux Footprint on Daytime Land-Atmosphere Coupling in Two Semiarid Ecosystems of the Southwestern U.S." *Water Resources Research* 52: 4785–4800. https://doi.org/10.1002/2015WR018016.

Archer, S., E. Andersen, K. I. Predick, S. Schwinning, R. Steidl, and S. Woods. 2017. "Woody Plant Encroachment: Causes and Consequences." In *Rangeland Systems: Processes, Management and Challenges.* Springer Series on Environmental Management, edited by D. Briske, 25–84. Cham: Springer. https://doi.org/10.1007/978-3-319-46709-2_2.

Beven, K. 2002. "Runoff Generation in Semi-Arid Areas." In *Dryland Rivers: Hydrology and Geomorphology of Semi-Arid Channels*, edited by L. J. Bull and M. J. Kirkby, 57–105. Chichester: Wiley & Sons.

Bracken, L. J., J. Wainwright, G. A. Ali, D. Tetzlaff, M. W. Smith, S. M. Reaney, and A. G. Roy. 2013. "Concepts of Hydrological Connectivity: Research Approaches, Pathways, and Future Agendas." *Earth-Science Reviews* 119: 17–34. https://doi.org/10.1016/j.earscirev.2013.02.001.

Dogra, K. S., S. K. Sood, P. K. Dobhal, and S. Sharma. 2010. "Alien Plant Invasion and Their Impact on Indigenous Species Diversity at Global Scale: A Review." *Journal of Ecology and the Natural Environment* 2: 175–186. https://doi.org/10.5897/JENE.9000012.

Galia, T., and V. Skarpich. 2017. "Response of Bed Sediments on the Grade-Control Structure Management of a Small Piedmont Stream." *River Research and Applications* 33(4): 483–494. https://doi.org/10.1002/rra.3111.

Gibbens, R. P., R. P. McNeely, K. M. Havstad, R. F. Beck, and B. Nolen. 2005. "Vegetation Changes in the Jornada Basin from 1858 to 1998." *Journal of Arid Environments* 61: 651–668. https://doi.org/10.1016/j.jaridenv.2004.10.001.

Goodrich, D. C., L. J. Lane, R. M. Shillito, S. N. Miller, K. H. Syed, and D. A. Woolhiser. 1997. "Linearity of Basin Response as a Function of Scale in a Semiarid Watershed." *Water Resources Research* 33: 2951–65. https://doi.org/10.1029/97WR01422.

Gutiérrez-Jurado, H. A., E. R. Vivoni, C. Cikoski, J. B. J. Harrison, R. L. Bras, and E. Istanbulluoglu. 2013. "On the Observed Ecohydrologic Dynamics of a Semiarid Basin with Aspect-Delimited Ecosystems." *Water Resources Research* 49: 8263–84. https://doi.org/10.1002/2013WR014364.

Gutiérrez-Jurado, H. A., E. R. Vivoni, E. Istanbulluoglu, and R. L. Bras. 2007. "Ecohydrological Response to a Geomorphically Significant Flood Event in a Semiarid Catchment with Contrasting Ecosystems." *Geophysical Research Letters* 34L: L24S25. https://doi.org/10.1029/2007GL030994.

Gwinn, R. W., and D. A. Parsons. 1976. "Discharge Equations for HS, H, and HL Flumes." *Journal of Hydraulic Division* 102(5): 11874–87.

Jencso, K. G., B. L. McGlynn, M. N. Gooseff, S. M. Wondzell, K. E. Bencala, and L. A. Marshall. 2009. "Hydrologic Connectivity between Landscapes and Streams: Transferring Reach- and Plot-Scale Understanding to the Catchment Scale." *Water Resources Research* 45(4): W04428. https://doi.org/10.1029/2008WR007225.

Kampf, S. K., J. Faulconer, J. R. Shaw, M. Lefsky, J. W. Wagenbrenner, and D. J. Cooper. 2018. "Rainfall Thresholds for Flow Generation in Desert Ephemeral Streams." *Water Resources Research* 54: 9935–50. https://doi.org/10.1029/2018WR023714.

Keller, Z. T. 2021. "Runoff Connectivity, Controls, and Evolution during the North American Monsoon." MS thesis, Arizona State University. 176 pp.

Leite, P. A. M., B. P. Wilcox, and K. J. McInnes. 2020. "Woody Plant Encroachment Enhances Soil Infiltrability of a Semiarid Karst Savanna." *Environmental Research Communications* 2: 115005. https://doi.org/10.1088/2515-7620/abc92f.

Ludwig, J. A., B. P. Wilcox, D. D. Breshears, D. J. Tongway, and A. C. Imeson. 2005. "Vegetation Patches and Runoff-Erosion as Interacting Ecohydrological Processes in Semiarid Landscapes." *Ecology* 86(2): 288–297. https://doi.org/10.1890/03-0569.

McKenna, O. P., and O. E. Sala. 2018. "Groundwater Recharge in Desert Playas: Current Rates and Future Effects of Climate

Change." *Environmental Research Letters* 13(1): 014025. https://doi.org/10.1088/1748-9326/aa9eb6.

Monger, H. C., and B. T. Bestelmeyer. 2006. "The Soil-Geomorphic Template and Biotic Change in Arid and Semi-Arid Ecosystems." *Journal of Arid Environments* 65: 207–218. https://doi.org/10.1016/j.jaridenv.2005.08.012.

Moody, J. A., D. A. Martin, S. L. Haire, and D. A. Kinner. 2008. "Linking Runoff Response to Burn Severity after a Wildfire." *Hydrological Processes* 22(13): 2063–74. https://doi.org/10.1002/hyp.6806.

Nearing, M. A., S. Yin, P. Borrelli, and V. O. Polyakov. 2017. "Rainfall Erosivity: An Historical Review." *Catena* 157: 357–362. https://doi.org/10.1016/j.catena.2017.06.004.

Newman, B. D., B. P. Wilcox, S. Archer, D. D. Breshears, C. N. Dahm, C. J. Duffy, N. G. McDowell, F. M. Phillips, B. R. Scanlon, and E. R. Vivoni. 2006. "The Ecohydrology of Arid and Semiarid Environments: A Scientific Vision." *Water Resources Research* 42: W06302. https://doi.org/10.1029/2005WR004141.

Nichols, M. H., and V. O. Polyakov. 2019. "The Impacts of Porous Rock Check Dams on a Semiarid Alluvial Fan." *Science of the Total Environment* 664: 576–582. https://doi.org/10.1016/j.scitotenv.2019.01.429.

Norman, L. M., R. Lal, E. Wohl, E. Fairfax, A. C. Gellis, and M. M. Pollock. 2022. "Natural Infrastructure in Dryland Streams (NIDS) Can Establish Regenerative Wetland Sinks that Reverse Desertification and Strengthen Climate Resilience." *Science of the Total Environment* 849: 157738. https://doi.org/10.1016/j.scitotenv.2022.157738.

Norman, L. M., J. B. Sankey, D. Dean, J. Caster, S. DeLong, W. DeLong, and J. D. Pelletier. 2019. "Quantifying Geomorphic Change at Ephemeral Stream Restoration Sites Using a Coupled-Model Approach." *Geomorphology* 283: 1–16. https://doi.org/10.1016/j.geomorph.2017.01.017.

Okin, G. S., M. Moreno-de las Heras, P. M. Saco, H. L. Throop, E. R. Vivoni, A. J. Parsons, J. Wainwright, and D. P. C. Peters. 2015. "Connectivity in Dryland Landscapes: Shifting Concepts of Spatial Interactions." *Frontiers in Ecology and the Environment* 13(1): 20–27. https://doi.org/10.1890/140163.

Okin, G. S., O. E. Sala, E. R. Vivoni, J. Zhang, and A. Bhattachan. 2018. "The Interactive Role of Wind and Water in Dryland Function: What Does the Future Hold?" *Bioscience* 68(9): 670–77. https://doi.org/10.1093/biosci/biy067.

Osborn, H. B., and L. Lane. 1969. "Precipitation-Runoff Relations for Very Small Semiarid Rangeland Watersheds." *Water Resources Research* 5(2): 419–425. https://doi.org/10.1029/WR005i002p00419.

Parsons, A. J., R. E. Brazier, J. Wainwright, and D. M. Powell. 2006. "Scale Relationships in Hillslope Runoff and Erosion." *Earth Surface Processes and Landforms* 31(11): 1384–93. https://doi.org/10.1002/esp.1345.

Pérez-Ruiz, E. R., E. R. Vivoni, and O. E. Sala. 2022. "Seasonal Carry-Over of Water and Effects on Carbon Dynamics in a Dryland Ecosystem." *Ecosphere* 13(7): e4189. https://doi.org/10.1002/ecs2.4189.

Peters, D. P. C., H. M. Savoy, S. Stillman, H. Huang, A. R. Hudson, O. E. Sala, and E. R. Vivoni. 2021. "Plant Species Richness in Multiyear Wet and Dry Periods in the Chihuahuan Desert." *Climate* 9(8): 130. https://doi.org/10.3390/cli9080130.

Polyakov, V. O., M. A. Nearing, M. H. Nichols, R. L. Scott, J. J. Stone, and M. P. McClaran. 2010. "Long-Term Runoff and Sediment Yields from Small Semiarid Watersheds in Southern Arizona." *Water Resources Research* 46: W09512. https://doi.org/10.1029/2009WR009001.

Puigdefabregas, J. 2005. "The Role of Vegetation Patterns in Structuring Runoff and Sediment Fluxes in Drylands." *Earth Surface Processes and Landforms* 30(2): 133–147. https://doi.org/10.1002/esp.1181.

Puigdefabregas, J., G. del Barrio, M. M. Boer, L. Gutierrez, and A. Sole. 1998. "Differential Responses of Hillslope and Channel Elements to Rainfall Events in a Semi-Arid Area." *Geomorphology* 23(2–4): 337–351. https://doi.org/10.1016/S0169-555X(98)00014-2.

Rango, A., K. Snyder, J. Herrick, K. Havstad, R. Gibbens, J. Wainwright, and T. Parsons. 2003. "Historical and Current Hydrological Research at the USDA/ARS Jornada Experimental Range in Southern New Mexico." In *First Interagency Conference on Research in the Watersheds*, edited by K. G. Renard, S. A. McElroy, W. J. Gburek, H. E. Canfield, and R. L. Scott, 302–7. Benson, AZ: USDA-ARS.

Rango, A., S. L. Tartowski, A. Laliberte, J. Wainwright, and A. Parsons. 2006. "Islands of Hydrologically Enhanced Biotic Productivity in Natural and Managed Arid Ecosystems." *Journal of Arid Environments* 65: 235–252. https://doi.org/10.1016/j.jaridenv.2005.09.002.

Reynolds, J. F., P. R. Kemp, K. Ogle, and R. J. Fernández. 2004. "Modifying the 'Pulse–Reserve' Paradigm for Deserts of North America: Precipitation Pulses, Soil Water, and Plant Responses." *Oecologia* 141(2): 194–210. https://doi.org/10.1007/s00442-004-1524-4.

Rossi, M. J., J. O. Ares, E. G. Jobbagy, E. R. Vivoni, R. W. Vervoot, A. P. Schreiner-McGraw, and P. M. Saco. 2018. "Vegetation and Terrain Drivers of Infiltration Depth along a Semiarid Hillslope." *Science of the Total Environment* 644: 1399–1408. https://doi.org/10.1016/j.scitotenv.2018.07.052.

Schlesinger, W. H., A. D. Abrahams, A. J. Parsons, and J. Wainwright. 1999. "Nutrient Losses in Runoff from Grassland and Shrubland Habitats in Southern New Mexico: I. Rainfall Simulation Experiments." *Biochemistry* 45(1): 21–34. https://doi.org/10.1023/A:1006020831706.

Schreiner-McGraw, A. P., and E. R. Vivoni. 2017. "Percolation Observations in an Arid Piedmont Watershed and Linkages to Historical Conditions in the Chihuahuan Desert." *Ecosphere* 8(11): e02000. https://doi.org/10.1002/ecs2.2000.

Schreiner-McGraw, A. P., and E. R. Vivoni. 2018. "On the Sensitivity of Hillslope Runoff and Channel Transmission Losses in Arid Piedmont Slopes." *Water Resources Research* 54(7): 4498–4518. https://doi.org/10.1029/2018WR022842.

Schreiner-McGraw, A. P., E. R. Vivoni, H. Ajami, O. E. Sala, H. L. Throop, and D. P. C. Peters. 2020. "Woody Plant Encroachment Is Expected to Have a Larger Impact Than Climate Change on Dryland Water Budgets." *Scientific Reports* 10: 8112. https://doi.org/10.1038/s41598-020-65094-x.

Seyfried, M. S., and B. P. Wilcox. 1995. "Scale and the Nature of Spatial Variability: Field Examples Having Implications for Hydrologic Modeling." *Water Resources Research* 31: 173–184. https://doi.org/10.1029/94WR02025.

Shanafield, M., and P. G. Cook. 2014. "Transmission Losses, Infiltration and Groundwater Recharge through Ephemeral and Intermittent Streambeds: A Review of Applied Methods." *Journal of Hydrology* 511: 518–529. https://doi.org/10.1016/j.jhydrol.2014.01.068.

Smith, R. W., D. L. Chery, K. G. Renard, and W. R. Gwinn. 1981. *Supercritical Flow Flumes for Measuring Sediment-Laden Flow*. Technical Bulletin No. 1655. Washington, DC: US Government Printing Office. 72 pp.

Stewart, J., A. J. Parsons, J. Wainwright, G. S. Okin, B. T. Bestelmeyer, E. L. Frederickson, and W. H. Schlesinger. 2014. "Modeling Emergent Patterns of Dynamic Desert Ecosystems." *Ecological Monographs* 84(3): 373–410. https://doi.org/10.1890/12-1253.1.

Stieglitz, M., J. Shaman, J. McNamara, V. Engel, J. Shanley, and G. W. King. 2003. "An Approach to Understanding Hydrologic Connectivity on the Hillslope and the Implications for Nutrient Transport." *Global Biogeochemical Cycles* 17(4): 1105. https://doi.org/10.1029/2003GB002041.

Templeton, R. C. 2011. "Insights on Seasonal Fluxes in a Desert Shrubland Watershed from a Distributed Sensor Network." MS thesis, Arizona State University. 171 pp.

Templeton, R. C., E. R. Vivoni, L. A. Méndez-Barroso, N. A. Pierini, C. A. Anderson, A. Rango, A. S. Laliberte, and R. L. Scott. 2014. "High-Resolution Characterization of a Semiarid Watershed: Implications on Evapotranspiration Estimates." *Journal of Hydrology* 509: 306–319. https://doi.org/10.1016/j.jhydrol.2013.11.047.

Tromble, J. 1988. "Water Budget for a Creosotebush-Infested Rangeland." *Journal of Arid Environments* 15(1): 71–74. https://doi.org/10.1016/s0140-1963(18)31006-1.

Turnbull, L., A. J. Parsons, and J. Wainwright. 2013. "Runoff Responses to Long-Term Rainfall Variability in a Shrub-Dominated Shrubland." *Journal of Arid Environments* 91: 88–94. https://doi.org/10.1016/j.jaridenv.2012.12.002.

Turnbull, L., A. J. Parsons, J. Wainwright, J. P. Anderson, and J. M. Tromble. 2020. "Streamflow and Rain Event Data from the Tromble Experimental Watershed Weir in the Jornada Basin, Southern New Mexico USA, during 2 Periods: 1977-1985 and 2003-2011 Ver. 1." Environmental Data Initiative. https://doi.org/10.6073/pasta/1ddf31fd56d97f4b2817b2e17d683bbc.

Vivoni, E. R., E. R. Pérez-Ruiz, Z. T. Keller, E. A. Escoto, R. C. Templeton, N. P. Templeton, C. A. Anderson, et al. 2021. "Long-Term Research Catchments to Investigate Shrub Encroachment in the Sonoran and Chihuahuan Deserts: Santa Rita and Jornada Experimental Ranges." *Hydrological Processes* 35: e14031. https://doi.org/10.1002/hyp.14031.

Vivoni, E. R., E. R. Pérez-Ruiz, A. P. Schreiner-McGraw, Z. Keller, R. C. Templeton, and C. A. Anderson. 2022. "Precipitation Data from Four Locations within the Tromble Weir Experimental Watershed, Located at the Jornada Basin LTER Site, 2010-Ongoing Ver. 23." Environmental Data Initiative. https://doi.org/10.6073/pasta/759f2f1bc29df9bd15a9a9bfd6a15470.

Vivoni, E. R., A. Rango, C. A. Anderson, N. A. Pierini, A. Schreiner-McGraw, S. Saripalli, and A. S. Laliberte. 2014. "Ecohydrology with Unmanned Aerial Vehicles." *Ecosphere* 5(10): art130. https://doi.org/10.1890/ES14-00217.1.

Wainwright, J. 2006. "Climate and Climatological Variations in the Jornada Basin." In *Structure and Function of Chihuahuan Desert Ecosystem: The Jornada Basin Long-Term Ecological Research Site*, edited by K. Havstad, L. F. Huenneke, and W. H. Schlesinger, 44–80. New York: Oxford University Press. https://doi.org/10.1093/oso/9780195117769.001.0001.

Wainwright, J., A. J. Parsons, W. H. Schlesinger, and A. D. Abrahams. 2002. "Hydrology-Vegetation Interactions in Areas of Discontinuous Flow on a Semi-Arid Bajada, Southern New Mexico." *Journal of Arid Environments* 51: 319–338. https://doi.org/10.1006/jare.2002.0970.

Wilcox, B. P., D. D. Breshears, and C. D. Allen. 2003. "Ecohydrology of a Resource-Conserving Semiarid Woodland: Effects of Scale and Disturbance." *Ecological Monographs* 73: 223–239. https://doi.org/10.1890/0012-9615(2003)073[0223:EOARSW]2.0.CO;2.

Wohl, E. 2006. "Human Impacts to Mountain Streams." *Geomorphology* 79(3–4): 217–248. https://doi.org/10.1016/j.geomorph.2006.06.020.

Wondzell, S. M., G. L. Cunningham, and D. Bachelet. 1996. "Relationships between Landforms, Geomorphic Processes, and Plant Communities on a Watershed in the Northern Chihuahuan Desert." *Landscape Ecology* 11(6): 351–362. https://doi.org/10.1007/BF02447522.

Yetemen, O., E. Istanbulluoglu, J. H. Flores-Cervantes, E. R. Vivoni, and R. L. Bras. 2015. "Ecohydrologic Role of Solar Radiation on Landscape Evolution." *Water Resources Research* 51(2): 1127–57. https://doi.org/10.1002/2014WR016169.

Zhou, X., E. Istanbulluoglu, and E. R. Vivoni. 2013. "Modeling the Ecohydrological Role of Aspect-Controlled Radiation on Tree-Grass-Shrub Coexistence in a Semiarid Climate." *Water Resources Research* 49(5): 2872–95. https://doi.org/10.1002/wrcr.20259.

How to cite this article: Keller, Zachary T., Enrique R. Vivoni, Charles R. Kimsal, Agustín Robles-Morua, and Eli R. Pérez-Ruiz. 2023. "Hillslope to Channel Hydrologic Connectivity in a Dryland Ecosystem." *Ecosphere* 14(11): e4707. https://doi.org/10.1002/ecs2.4707